Determination of optical properties of human blood in the spectral range 250 to 1100 nm using Monte Carlo simulations with hematocrit-dependent effective scattering phase functions

Moritz Friebel
Laser- und Medizin- Technologie GmbH, Berlin
Fabeckstr. 60-62
14195 Berlin, Germany

André Roggan
Gerhard Müller
Martina Meinke
Charité-Universitätsmedizin Berlin
Campus Benjamin Franklin
Institut für Medizinische Physik und Lasermedizin
Fabeckstr. 60-62
14195 Berlin, Germany
E-mail: martina.meinke@charite.de

Abstract. The absorption coefficient μ_a, scattering coefficient μ_s, and anisotropy factor g of diluted and undiluted human blood (hematocrit 0.84 and 42.1%) are determined under flow conditions in the wavelength range 250 to 1100 nm, covering the absorption bands of hemoglobin. These values are obtained by high precision integrating sphere measurements in combination with an optimized inverse Monte Carlo simulation (IMCS). With a new algorithm, appropriate effective phase functions could be evaluated for both blood concentrations using the IMCS. The best results are obtained using the Reynolds-McCormick phase function with the variation factor $\alpha = 1.2$ for hematocrit 0.84%, and $\alpha = 1.7$ for hematocrit 42.1%. The obtained data are compared with the parameters given by the Mie theory. The use of IMCS in combination with selected appropriate effective phase functions make it possible to take into account the nonspherical shape of erythrocytes, the phenomenon of coupled absorption and scattering, and multiple scattering and interference phenomena. It is therefore possible for the first time to obtain reasonable results for the optical behavior of human blood, even at high hematocrit and in high hemoglobin absorption areas. Moreover, the limitations of the Mie theory describing the optical properties of blood can be shown.
[DOI: 10.1117/1.2203659]

Keywords: optical properties; blood; absorption coefficient; scattering coefficient; anisotropy factor; effective phase function; Monte Carlo simulation.

Paper 05264R received Sep. 14, 2005; revised manuscript received Dec. 21, 2005; accepted for publication Feb. 21, 2006; published online May 24, 2006.

1 Introduction

A basic understanding of the light-scattering and absorption properties of human blood is of increasing interest for a number of medical applications and for diagnostic purposes. The description of the optical behavior of human blood is a complex task: light is absorbed and scattered by the discoid-shaped erythrocytes. This optical behavior is a result of the highly concentrated hemoglobin content of the cell. The hemoglobin causes a higher real part of the refractive index compared to the surrounding plasma.[1] Hemoglobin shows distinct absorption peaks in the visible range, leading to increased values in the imaginary part.[1] As a consequence, absorption can only take place within the cell and is not independent of the scattering. Furthermore, the theoretical mean distance between cells in blood of physiological concentration is of the order of their diameter. Under flow conditions, the red blood cells tend to be more highly concentrated in the central part of the flow, leading to deviations of local values of the hematocrit (Hct) from the bulk value, which is routinely determined for human blood. Therefore, the distance between the cells becomes smaller in the center, and the cells can even be in contact with one another. Therefore interfering waves from neighboring cells cannot be neglected. In addition, absorption, shape, volume, alignment, and aggregation of these cells changes with a number of other physiological parameters such as oxygen saturation,[2] shear rate,[3–5] or osmolarity.[2,6]

As a result, it is difficult to describe the optical behavior of blood under these various conditions using analytical models such as the Mie theory, because of the absence of theoretical preconditions or their lack of flexibility. The double integrating sphere technique combined with inverse Monte Carlo simulation (IMCS) has been established[2,7] as a useful means of determination of the optical parameters of undiluted blood. Integrating sphere measurements of undiluted blood in the wavelength range of 400 to 570 nm are problematic, because the high concentration of scattering cells combined with high

Address all correspondence to Martina Meinke, Charité-Universitätsmedizin Berlin, Campus Benjamin Franklin, Institut für Medizinische Physik und Lasermedizin, Fabeckstr. 60-62, 14195 Berlin, Germany. Tel: 49–30–844 54158; Fax: 49–30–844 51289; E-mail: martina.meinke@charite.de

1083-3668/2006/11(3)/034021/10/$22.00 © 2006 SPIE

absorption complicates the detection of ballistic photons, even when very thin samples and highly intense light sources are used. The ballistic photons are normally one of the three independent macroscopic measurement parameters.

According to the transport theory, the optical properties of blood can be described by the intrinsic optical parameters absorption coefficient μ_a, scattering coefficient μ_s, and anisotropy factor g. The IMCS calculates the photon trajectories on the basis of a given phase function that describes the statistical angle distribution of a scattering event. For the description of the optical behavior of flowing blood, it is necessary to determine the appropriate effective phase function that allows the description of the real radiation distribution within the investigated medium,[8] including the phenomena of coupled absorption and scattering, multiple scattering, or form factors of the erythrocytes and their inhomogeneous local distribution within the flow stream.

Several goniometric measurements of single cells or highly diluted blood samples with a very thin sample thickness have been carried out to evaluate phase functions for the single red blood cell.[9,10] It is clear that single scattering of individual red blood cells cannot be extrapolated for the scattering of blood[11] of physiological concentration. An effective phase function may depend on the hematocrit and wavelength, especially at high absorption. There the reflection is increased, induced by the increase in the complex refractive index, and the transmission is decreased by increased absorption within the cell. Moreover, some investigations indicate that in the case of high hematocrit levels, the scattering anisotropy of red blood cells is strongly influenced by the flow conditions[12–14] particularly the shear-rate-dependent aggregation and disaggregation phenomena[4,15–17] Although there are a number of further studies about the optical parameters of blood,[2,3,18–20] there is only limited information available about the effective phase function of undiluted blood,[21] and only for single wavelengths.

Most of the reported measurements of the intrinsic optical parameters of blood fail to determine μ_s and g independently, and present only the effective scattering coefficient μ_s'. Although the behavior of μ_s and g of whole blood at increasing absorption is of special physical interest for a better understanding of the interaction between the electromagnetic wave and the densely packed erythrocytes, there is almost no data available at the wavelengths where the absorption of hemoglobin is high.

This work presents an evaluation of the effective phase functions of diluted and undiluted flowing blood in the spectral range of 250 to 1100 nm, including the regions of high absorption. The flow conditions within the cuvettes should correspond to those in arterioles of comparable diameters. This was realized by keeping a constant wall shear rate, where the shear rate decreases, depth dependent, toward the center of the cuvette. Aggregation phenomena could not be examined because washed erythrocyte suspensions were investigated.

Using the evaluated effective phase functions, all the parameters, i.e., absorption coefficient μ_a, scattering coefficient μ_s, and anisotropy factor g of blood for Hct 0.84 and 42.1%, could be determined independently at any wavelength. These were obtained by high precision integrating sphere[22] measurements of diffuse reflectance, total transmission, and not only of ballistic photons but also of the collimated transmission within an aperture of 5.3 deg. The collimated transmission was increased by using extremely thin samples, down to 40 μm. An optimized IMCS based on Roggan et al.,[23] which simulates the exact geometry of the experimental setup including all kinds of radiation losses, was used with an error threshold of 0.05%.

Inverse Monte Carlo simulations generally do not have this precision. Yaroslavsky et al.,[8] for example, showed the importance of the right phase function by comparing the intrinsic parameters of undiluted blood simulated with both Henyey-Greenstein and Reynolds-McCormick (variation factor $\alpha=1$) phase functions with error thresholds of 0.5%. This led to a successful simulation with μ_s values of 40 and 413 mm^{-1}, respectively, which is a rather large range. The optimized IMCS with reduced error threshold used in this work would not accept the use of two quite different phase functions for the same simulation dataset.

The determined intrinsic optical parameters of diluted and undiluted blood were compared with data calculated by the Mie theory.

2 Material and Methods

2.1 *Blood Preparation*

Fresh human erythrocytes from a healthy blood donor were centrifuged three times and washed with isotonic phosphate buffer (300 mosmol/L, pH 7.4) to remove the blood plasma and free hemoglobin. The hematocrit was varied by diluting the sample with buffer to values 0.84 and 42.1%, which correspond to hemoglobin solution values of 0.27 and 12.9 g/dL, respectively. The hematocrit under static conditions was determined using a red blood cell counter (Micros 60 OT 18, ABX Diagnostics, Montpellier, France), and the oxygen saturation was measured with a blood gas analyzer (OPTI Care, AVL Medizintechnik GmbH, Bad Homburg, Germany). A miniaturized blood circulation setup was adapted with a roller pump (Stöckert Instruments GmbH, München, Germany) and a blood reservoir, which was constantly aerated with a gas mixture of O_2, N_2, and CO_2 to maintain both the oxygen saturation ($>99\%$) and a constant pH (7.4). The temperature was kept constant at 20 °C. The blood was gently stirred within the reservoir to avoid creating concentration inhomogenities caused by sedimentation or cell aggregation. The blood was kept flowing by a specially designed, turbulence-free cuvette with a laminar flow and a sample thickness of 1020 and 116 μm for Hct 0.84 and 42.1%, respectively, which imitates the flow conditions in arterioles of similar diameters. The flow was regulated for each sample thickness to a constant wall shear rate of 600 s^{-1} at the cuvette windows. The shear rate decreases to values approaching zero at the center of the cuvette. Thus, the direction of the incident light was parallel to the velocity gradient. For additional measurements in the wavelength region at 415 nm where the hemoglobin absorption is very high, a cuvette was used with a sample thickness of 40 μm.

2.2 *Experimental Setup*

The macroscopic optical parameters, diffuse reflectance R_d, the total transmission T_t, and the diffuse transmission T_d

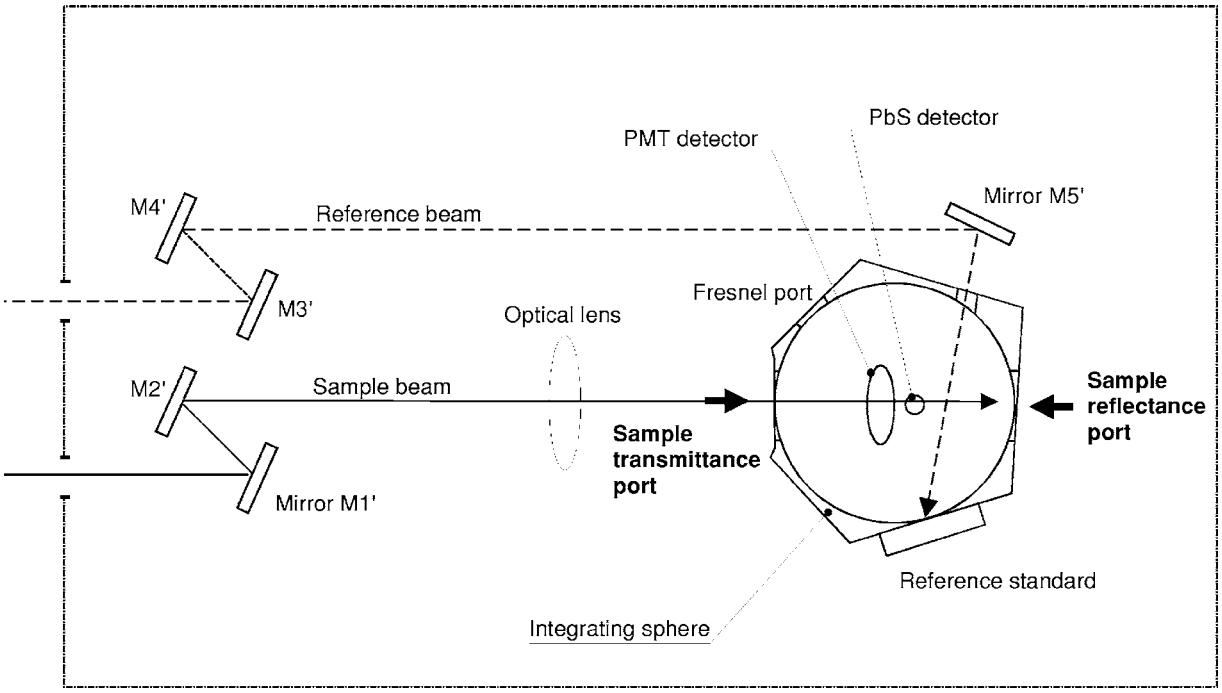

Fig. 1 Schematic diagram of the integrating sphere spectrometer. The reference beam goes via mirrors M3 to M5 into the integrating sphere. The sample beam reaches the sample via mirrors M1 and M2.

(=T_t—transmission within an aperture of 5.3 deg) of flowing blood were measured every 5 nm in the spectral range from 250 to 1100 nm using an integrating sphere spectrometer (Lambda 900, PerkinElmer, Rodgau-Jügesheim, Germany), which is a two-beam spectrometer with double monochromator system (Fig. 1). The light source consists of a deuterium lamp for the UV range and a wolfram halogen lamp for the visible/near infrared (NIR) range. The light intensity was adapted to the absorption behavior of the sample to maintain the intensity of the signal in the optimal range of the detectors. This optical arrangement of a sample and a reference beam compensates for light intensity shifts, and changes in the inner sphere reflectivity by positioning the glass cuvette onto the sphere. The cuvette can be fixed in defined position at a constant distance to the sphere aperture, in front of or behind the integrating sphere, to measure the transmittance or reflectance spectra. For the measurement of T_t the reflectance port is closed with a diffuse reflecting Spectralon® standard. T_d is measured after the standard is removed, so that nonscattered and scattered transmitted light leaves the sphere within an angle of 5.3 deg. R_d is measured relative to the reflectance standard by replacing the special Spectralon® standard with a certified, known reflectance spectrum by the sample that is inclined at an angle of 8 deg to the incoming light. The Fresnel reflectance of the cuvette glass leaves the sphere through the open Fresnel port to avoid interference with the diffuse reflectance. This experimental setup allows the measurement of macroscopic radiation distribution with an extremely reduced error potential. The accuracy of repetitive measurements of the reflectance and transmission measurements of a sample with defined optical properties (e.g., polystyrene spheres) was smaller than 0.01%. Measurements on flowing blood resulted in an accuracy of 0.02%, probably induced by flow-dependent local inhomogenities in the Hct.

2.3 *Principle of Inverse Monte Carlo Simulation*

The IMCS method, which was first presented by Roggan et al.[23] could be well adapted to the geometry of the measurement system. The IMCS, shown schematically in Fig. 2, uses forward Monte Carlo simulations iteratively to calculate optical parameters μ_a, μ_s, and g on the basis of a given phase function and measured values R_d^M, T_t^M, and T_d^M for reflection and transmission. The forward simulation used in the present study considers all kinds of radiation losses within the experimental setup, including the simulation of the exact geometry of the sample and the cuvette, the integrating sphere, the illuminating light beam, and all the diaphragms and apertures. A precise consideration of the radiation losses reduces the error with respect to the determination of the intrinsic parameters to a minimum.

The IMCS presented here applies the Newton-Raphson method[24] to find an approximate solution of the nonlinear system of Eq. (1),

$$R_d(\mu_a,\mu_s,g) = R_d^M$$

$$T_t(\mu_a,\mu_s,g) = T_t^M$$

$$T_d(\mu_a,\mu_s,g) = T_d^M, \tag{1}$$

where the quantities on the left are the result of the forward simulation.

As a starting value for the Newton-Raphson method, an estimation of the parameters μ_a, μ_s, and g from the Kubelka-

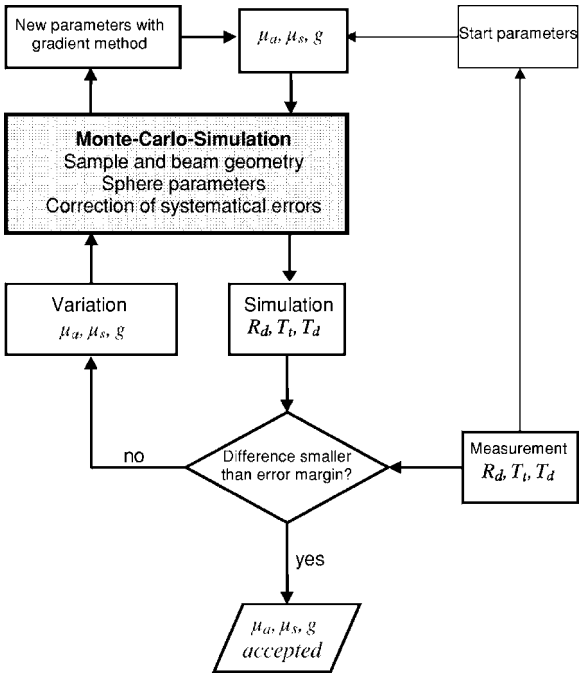

Fig. 2 Flow chart of the inverse Monte Carlo simulation.

Munk theory is used. The calculated R_d^S, T_t^S, and T_d^S are then compared to measured values R_d^M, T_t^M, and T_d^M,

$$\Delta R_d^{\mathrm{MS}} = R_d^M - R_d^S$$

$$\Delta T_t^{\mathrm{MS}} = T_t^M - T_t^S$$

$$\Delta T_c^{\mathrm{MS}} = T_c^M - T_c^S. \tag{2}$$

In the case of a significant deviation in Eq. (2), the gradient matrix (Jacobian matrix) for the set of functions R_d, T_t, and T_d is calculated approximately with finite differences obtained by forward simulations using slightly varied parameters. Then, according to the Newton-Raphson method, a refined approximation of the optical parameters is calculated by solving the following linear set of Eq. (3):

$$\begin{pmatrix} \frac{\partial R_d^S}{\partial \mu_a} & \frac{\partial R_d^S}{\partial \mu_s} & \frac{\partial R_d^S}{\partial g} \\ \frac{\partial T_t^S}{\partial \mu_a} & \frac{\partial T_t^S}{\partial \mu_s} & \frac{\partial T_t^S}{\partial g} \\ \frac{\partial T_c^S}{\partial \mu_a} & \frac{\partial T_c^S}{\partial \mu_s} & \frac{\partial T_c^S}{\partial g} \end{pmatrix} * \begin{pmatrix} \Delta\mu_a \\ \Delta\mu_s \\ \Delta g \end{pmatrix} = \begin{pmatrix} \Delta R_d^{MS} \\ \Delta T_t^{MS} \\ \Delta T_c^{MS} \end{pmatrix}. \tag{3}$$

Depending on the number of photons and the values of μ_a and μ_s, one forward simulation can take from a half to five minutes (Pentium processor with 400 MHz). The Newton-Raphson procedure was repeated until the deviation between measured and calculated R_d, T_t, and T_d values was within the given error threshold. For the calculation of the optical parameters by a known phase function, 10 to 20 iterations were used on average (error threshold 0.1%). A total inversion process of such a calculation took 5 to 30 min. This was repeated for all investigated wavelengths.

2.4 *Possibility of Determination of the Intrinsic Parameters*

The found intrinsic parameters can be seen as the optical properties of the sample, with the prerequisite that the transformation function $f(\mu_a, \mu_s, g) => (R_d, T_t, T_d)$ is in one-to-one correspondence. This underlying transformation function is *a priori* unknown and depends not only on the phase function but also on the geometric position of the detectors, the geometry of the illuminating light beam, the geometry and the optical properties of the sample, and as a consequence, also on the wavelength. Therefore the one-to-one correspondence must be evaluated over the whole spectral range. Also, the propagation of the errors in the measurement of R_d, T_t, and T_d into the resulting errors of the determined μ_a, μ_s, and g is not directly predictable. Spectral ranges can exist where the system is underdetermined, making it impossible, for example, to determine μ_s and g independently. In special cases, the one-to-one correspondence could be investigated by systematically searching for other μ_s and g pairs of identical μ_s' values, with which the IMCS remains below the error threshold. In all simulations presented in this study, there is no indication that an invalid one-to-one correspondence occurred at any time.

The high precision of the intensity measurement combined with the high resolving simulation leads to the system registering small deviations in the specified boundary condition. Examples of significant boundary conditions are the refractive index of the cuvette glass or the space between cuvette and aperture of the integrating sphere. Under certain conditions, such as special wavelength ranges, sample properties, and geometries, the spatial distribution of the radiation losses can influence the measured R_d, T_t, and T_d values significantly. This means additional information is registered. As a consequence, with this system it is possible, for example, to find a reasonable set of μ_a, μ_s, and g values even when T_d is equal to T_t, i.e., there are only two independent measurement parameters. Furthermore, it is possible using all three measurement parameters to evaluate the most appropriate effective phase function that leads to the lowest error or gives the most successful simulations at a fixed error threshold.

This IMCS makes it possible to compare different phase functions such as Mie[25] and Henyey-Greenstein,[26] or to fit an adaptable phase function to the optimal form such as the Reynolds-McCormick phase function with the variation factor α, as shown in this work.

Equation (4) shows the Reynolds-McCormick phase function:

$$p_{GK}(\mathbf{s},\mathbf{s}') = \alpha\hat{g}\frac{1}{\pi}\frac{(1-\hat{g}^2)^{2\alpha}}{[(1+\hat{g})^{2\alpha}-(1-\hat{g})^{2\alpha}](1+\hat{g}^2-2\hat{g}\cos\Theta)^{(\alpha+1)}}, \tag{4}$$

where $\alpha > -0.5$ and $|\hat{g}| \leqslant 1$ is a parameter from which the anisotropy factor g (mean cosine of scattering angle Θ) can be calculated. $p(\mathbf{s},\mathbf{s}')$ is the probability of scattering a photon

with the direction **s** to the direction **s′**, where Θ is the angle between **s** and **s′**.

2.5 *Measurement Performance*

Different phase functions and their dependence on wavelength and hematocrit were investigated to evaluate the most appropriate effective phase function. A very time-consuming fit procedure (two to four weeks for five wavelengths) was used with a possible total of 36 variation cycles and up to 10^8 photons per fit step with no given error threshold. The lowest deviation that could be reached by the simulation within a defined number of fit and variation steps indicates the most appropriate effective phase function. The R_d, T_t, and T_d values of five selected wavelengths for the two different hematocrits were used for the simulation.

In a second step, a procedure that uses less simulation time (up to one week for the 171 wavelengths) but offers higher precision was established to determine the effective phase function. The procedure results in one effective phase function for the regarded wavelength range, assuming that the phase function is independent of the wavelength. The IMCS was carried out using Reynolds-McCormick phase functions with different α values for the two hematocrits to find the best phase function for the entire spectral range between 250 and 1100 nm. R_d, T_t, and T_d were measured every 5 nm resulting in 171 datasets that had to be simulated by IMCS. To reduce the calculation expense, the threshold for the error of each of the three fitted signals was set to 0.05%, i.e., 10^6 to 10^7 start photons were calculated in each fit step. During the fitting procedure, the number of photons was increased dynamically according to the precision required. If the simulation was unable to find a solution for the three intrinsic optical parameters of a measured R_d, T_t, and T_d dataset at a single wavelength, the calculation was stopped, the dataset marked with "error," and the next μ_a, μ_s, and g set was simulated. The final number of failed simulations occurring for the whole spectrum (171 wavelengths) was counted for each simulation, dependent on the variation factor α.

As described in Sec. 2.3, an error threshold of 0.1% was used for the simulation of the intrinsic optical parameters of blood using the determined effective phase functions. For both hematocrits, a total of three independent measurement series were carried out and independently simulated.

3 Results and Discussion

3.1 *Investigation of Different Phase Functions Depending on Wavelength and Hematocrit*

Different phase functions were tested such as the Reynolds-McCormick (RM) phase function, the Henyey-Greenstein (HG), and the modified HG phase function. The IMCS without error threshold was applied to averaged datasets of R_d, T_t, and T_d at 300, 415, 575, 700, and 900 nm for blood with Hct 0.84 and 42.1%. The best results were obtained with the Reynolds-McCormick phase function. Figure 3 shows the sum of the minimal absolute percentage deviation of R_d, T_t, and T_d for Hct 0.84% for the five wavelengths depending on α, ranging from 0.5 to 3. Values of α smaller than 0.5 and higher than 3 lead to much higher errors and are not shown. The data show no indication of significant wavelength dependence within this range. No wavelength dependence was obtained for Hct 42.1% either. With regard to the mean values, the optimal value of α appears to be in the range between 1 and 2 for diluted and undiluted blood.

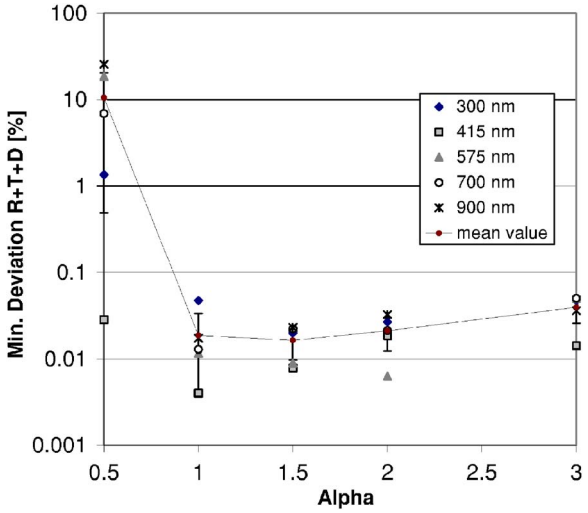

Fig. 3 Sum of the minimal absolute percentage deviation of R_d, T_t, and T_d for Hct 0.84% for selected wavelengths and its mean values dependent on variation factor α ranging from 0.5 to 3.

3.2 *Precise Evaluation of the Reynolds-McCormick Phase Function Depending on Hematocrit*

Due to wavelength independence, the more precise procedure could be used to determine the effective phase function. Figure 4 shows the absolute number of datasets of the 171 in the wavelength range 250 to 1100 nm that could not be successfully simulated dependent on α for Hct 0.84 and 42.1%. From these curves it can be deduced that the Reynolds-McCormick (RM) phase function with α between 1.2 and 1.3 is the best effective phase function for describing the real scattering behavior of flowing blood with Hct 0.84%. For undiluted blood with Hct 41.2%, the best effective phase function can be obtained with α between 1.6 and 1.8.

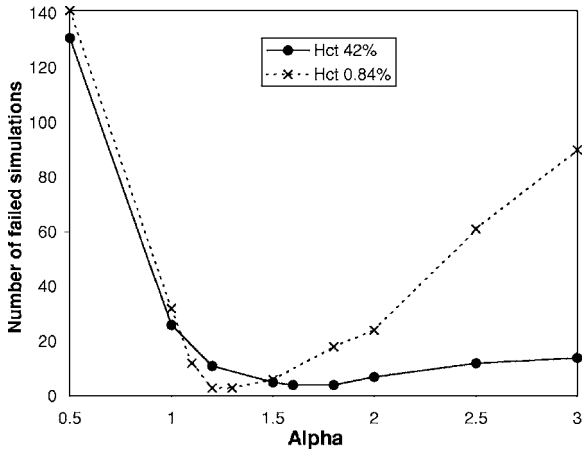

Fig. 4 Absolute number of unsuccessfully simulated datasets for nine simulations with different α values.

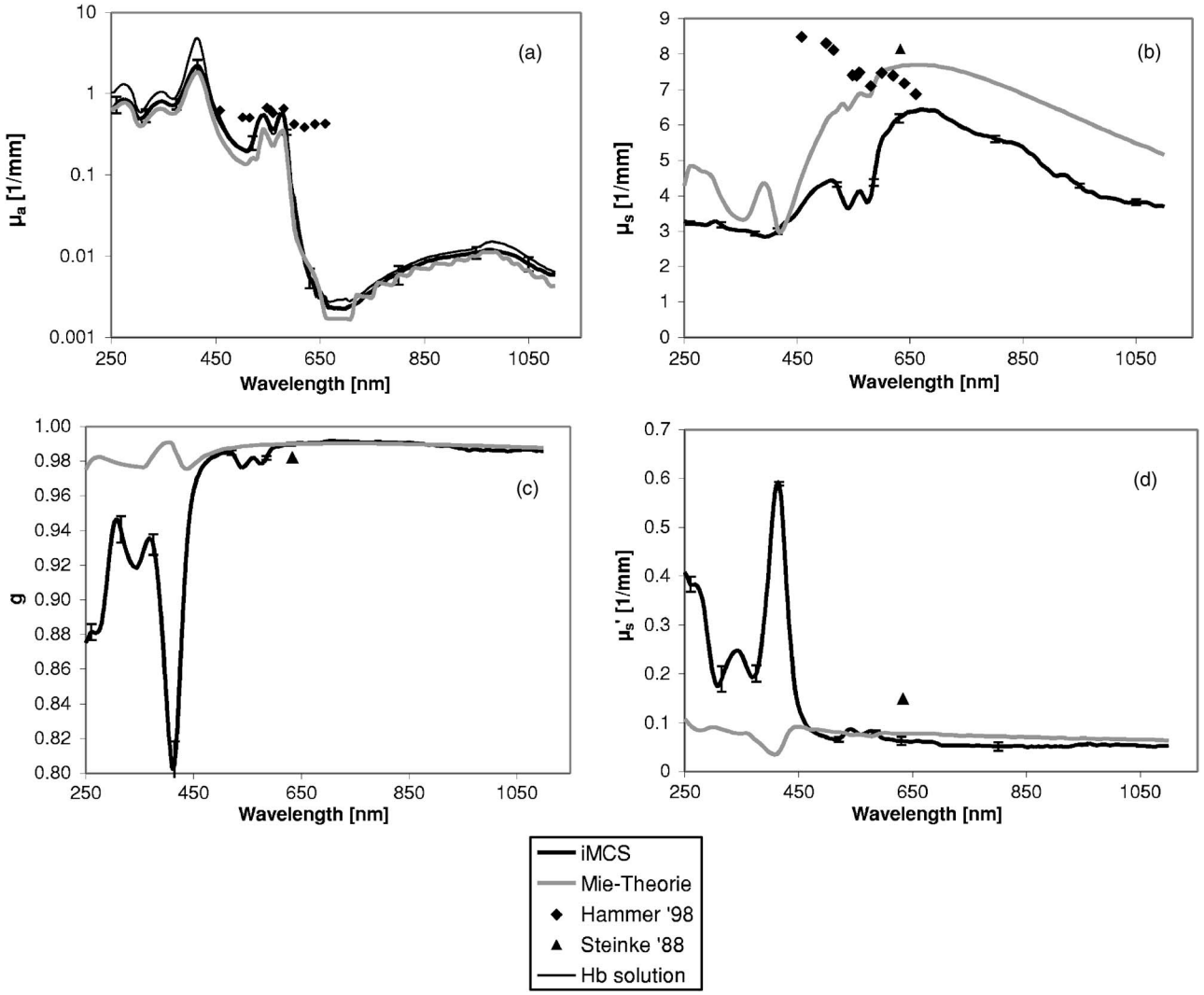

Fig. 5 (a) Absorption coefficient μ_a, (b) scattering coefficient μ_s, (c) anisotropy factor g, and (d) reduced scattering coefficient μ_s' of flowing red blood cells (wall shear rate 600 s^{-1}) with a hematocrit value of 0.84% in the wavelength range 250 to 1100 nm, compared to μ_a of a hemoglobin solution (0.27 g/dL), to values calculated by the Mie theory and to data from the literature.[9,19]

For the diluted blood, the result is in agreement with data from Yaroslavsky et al.[10] and Hammer et al.[9] obtained by goniometric measurements, indicating that the optimal α is 1 and 1.5, respectively. Hammer et al.[9] also found the RM-phase function to be wavelength independent in the range 489 to 690 nm. However, the α value for undiluted blood is in contrast to the results presented by Hammer et al.,[21] who found the optimal effective phase function with α=0.49 (HG phase function) at 514 nm. Using the HG phase function in the Monte Carlo simulation used in this work allows no successful simulation at 514 nm and leads to 77% error datasets for the wavelength range 250 to 1100 nm.

3.3 *Optical Parameters of Diluted Blood*

Using the evaluated Reynolds-McCormick phase functions with α=1.25 for blood with Hct 0.84% and 1.7 for blood with Hct 42.1%, the absorption coefficient μ_a, the scattering coefficient μ_s, and the anisotropy factor g were determined in the wavelength range 250 to 1100 nm. Figure 5 shows the spectra of μ_a, μ_s, g, and μ_s' as mean values of the simulation of three different R_d, T_d, and T_t measurements compared with literature data and data calculated using the Mie theory for spherical scatterers of the same mean volume and complex refractive index as the measured erythrocytes. Where necessary, the literature data were rescaled. The error bars are standard deviations (SD) for selected wavelengths. For μ_a, the mean relative SD averaged over all 171 wavelengths is 1.9%, ranging from 0.06 to 8%. The mean SD for μ_s and g is 0.85% (0.06 to 4.8%) and 0.036% (0.001 to 0.26%), respectively, leading to a mean SD of 1.6% for μ_s' (0.11 to 28.8%). For μ_a, the spectrum of a hemoglobin (Hb) solution of the same Hb content is also shown. The absorption spectrum shows the typical maxima of oxygenated Hb at 415 nm and the double peak at 540 and 575 nm. The Mie curve is comparable to the measured absorption in the range of low absorption above 600 nm. At higher absorptions, Mie values are lower with a maximal difference of about 30% in the range around 500 nm. The absorption of the Hb solution shows only dis-

tinctly higher values at the highest μ_a peaks. If absorption decreases, the difference between the μ_a values of the Hb solution and blood decreases. This can be explained by the Sieve effect. When light passes through a suspension of absorbing particles, such as blood, photons that do not encounter red blood cells pass unattenuated by absorption. As a consequence, the transmitted light intensity is higher than it would be if all the hemoglobin were uniformly dispersed in the solution. The magnitude of this effect increases with increasing μ_a and decreasing Hct.[27] This phenomenon is also known as "absorption flattening," because the heights of peaks in an absorption spectrum for a suspension are depressed relative to those for a homogeneous solution of the same average concentration. This describes exactly the effect observed in Fig 5. The spectrum of the scattering coefficient shows, in principle, a similar shape to that calculated by the Mie theory but is on average 22% lower, dependent on the wavelength. The values of Hammer et al.[21] using the anomalous diffraction theory do not appear to give better agreement.

The anisotropy factor g between 600 and 1100 nm is in the range of 0.99 and is identical to that calculated with the Mie theory. The Mie curve is obtained using the complex refractive index of hemoglobin[28] and shows at 415 nm the typical shape corresponding to the refractive index and indicates anomalous dispersion. The g value of 0.9818 determined by Steinke and Sheperd[19] at 633 nm for blood of a similar concentration is distinctly lower. Below 600 nm, the measured values start to decrease compared to the Mie theory. The curve of g seems to be inversely related to the absorption spectrum, leading to a distinct minimum of 0.805 at 415 nm. That means that the anisotropy factor at this Hct can be only described by the Mie theory if the hemoglobin absorption is very low.

The μ_s' spectrum is in principle the mirror image of the g spectrum. Analogous to μ_s, the effective scattering coefficient μ_s' in the range 460 to 1100 nm is on average 24% lower than the Mie theoretical values. Below 460 nm, the influence of the strongly decreasing g factor becomes dominant and μ_s' increases similarly, far above the values given by the Mie theory. There is currently no other data available in this high absorption region.

3.4 *Optical Parameters of Blood in Physiological Concentration*

Figure 6 shows the spectra of μ_a, μ_s, g, and μ_s' as mean values of the simulation of three different R_d, T_t, and T_d measurements for Hct 42.1% compared to the literature data and the Mie theory. Where necessary, the literature data were rescaled to Hct 42.1%. Equivalent to Fig. 5, the error bars are standard deviations (SD) for selected wavelengths. For μ_a, the mean relative SD is 3.1%, ranging from 0.03 to 42.9%. The mean SD for μ_s and g is 3.9% (0.012 to 39.5%) and 0.44% (0.001 to 8.7%), respectively, leading to a mean SD of 2.54% for μ_s' (0.006 to 29.6%). For μ_a, the spectrum of an Hb solution at the same Hb concentration is also shown. The relative differences between the measured spectra and the Mie curve are very similar to the ones at Hct 0.84%, indicating that the dependence of μ_a on the Hct is linear and independent of the wavelength. Compared to the measurements of Hct 0.84%, the μ_a peaks of blood and the Hb solution show a similar difference, indicating an unchanged Sieve effect in contrast to the expected decrease at increased Hct. Only in the range below 400 nm is the difference smaller. The highest μ_a value is reached at 415 nm with 105.9 mm^{-1}. Note that in contrast to the Sieve effect, all μ_a data from the literature[2,7,21] (all values determined with IMCS with exception of Reynolds[18]) are higher than the absorption spectrum of the Hb solution of the same Hb content. This could be explained by the previously discussed problem of determination of light losses in the IMCS. If some of the losses in radiation are neglected, the consequence would be an overestimation of μ_a.

As discussed for the diluted blood, the spectrum of the scattering coefficient of undiluted blood shows in principle a similar form to the curve given by the Mie theory. This was obtained from the Mie scattering cross section σ_s using the approximation equation[29] $\mu_s = \mathrm{Hct}(1-\mathrm{Hct})(\sigma_s/V)$, where V is the volume of the scatterer. However, depending on wavelength, the measured values are on average 59% lower, indicating that the prerequisite of independent scattering without interference phenomena is gradually eliminated by the decrease in the mean distances between the cells as discussed by Faber et al.[20] The data of Yaroslavsky et al.[7] Reynolds,[18] and Roggan et al.[2] confirms the measurements presented here in contrast to the Mie theoretical values. An exception to this is Hammer et al.[21] who presented data at 514 nm, even higher than the value given by the Mie theory.

In contrast to the diluted blood, the anisotropy factor g is distinctly lower than the Mie theoretical g values in the wavelength range 600 to 1100 nm, and no value is above 0.97. In a similar way to the spectrum of the diluted blood, the measured values start to decrease in contrast to the Mie theory below 600 nm, and the decrease is also related to the absorption spectrum but is more pronounced, leading to a minimum of 0.66 at 415 nm. The values of Hammer et al.[21] at 514 nm and Roggan et al.[2] at 633 nm are in good agreement with the simulated data. However, the data of Reynolds[18] and Yaroslavsky et al.[7] at 810, 960, and 1064 nm is in agreement with the Mie theory.

In the range of 600 to 1100 nm, the effective scattering coefficient μ_s' agrees well with the Mie theory with values between 1.9 and 2.27 mm^{-1}. Below 600 nm, μ_s' shows distinct maxima corresponding to the minima of the anisotropy factor and is up to 12 times (415 nm) higher than values calculated with the Mie theory. The data presented by Roggan et al.[2] (flowing blood, IMCS) and Enejder et al.[4] (flowing bovine blood, IMCS) is in good agreement with the data shown here, whereas the data of Yaroslavsky et al.[7] (IMCS) and Reynolds[18] at 810, 960, and 1064 nm is much lower (0.5 to 0.7 mm^{-1}). Hammer et al.[21] (angle-resolved MCS) determined μ_s' with 6.18 mm^{-1} at 514 nm, which is 2.38 times higher than the values presented in this work.

3.5 *General Discussion*

3.5.1 *Evaluation of the Phase Function*

The Reynolds-McCormick phase function has been identified as an appropriate effective phase function of blood, being dependent on cell concentration. However, no evidence was found for dependence on wavelength within the observed range for both of the investigated blood concentrations. This

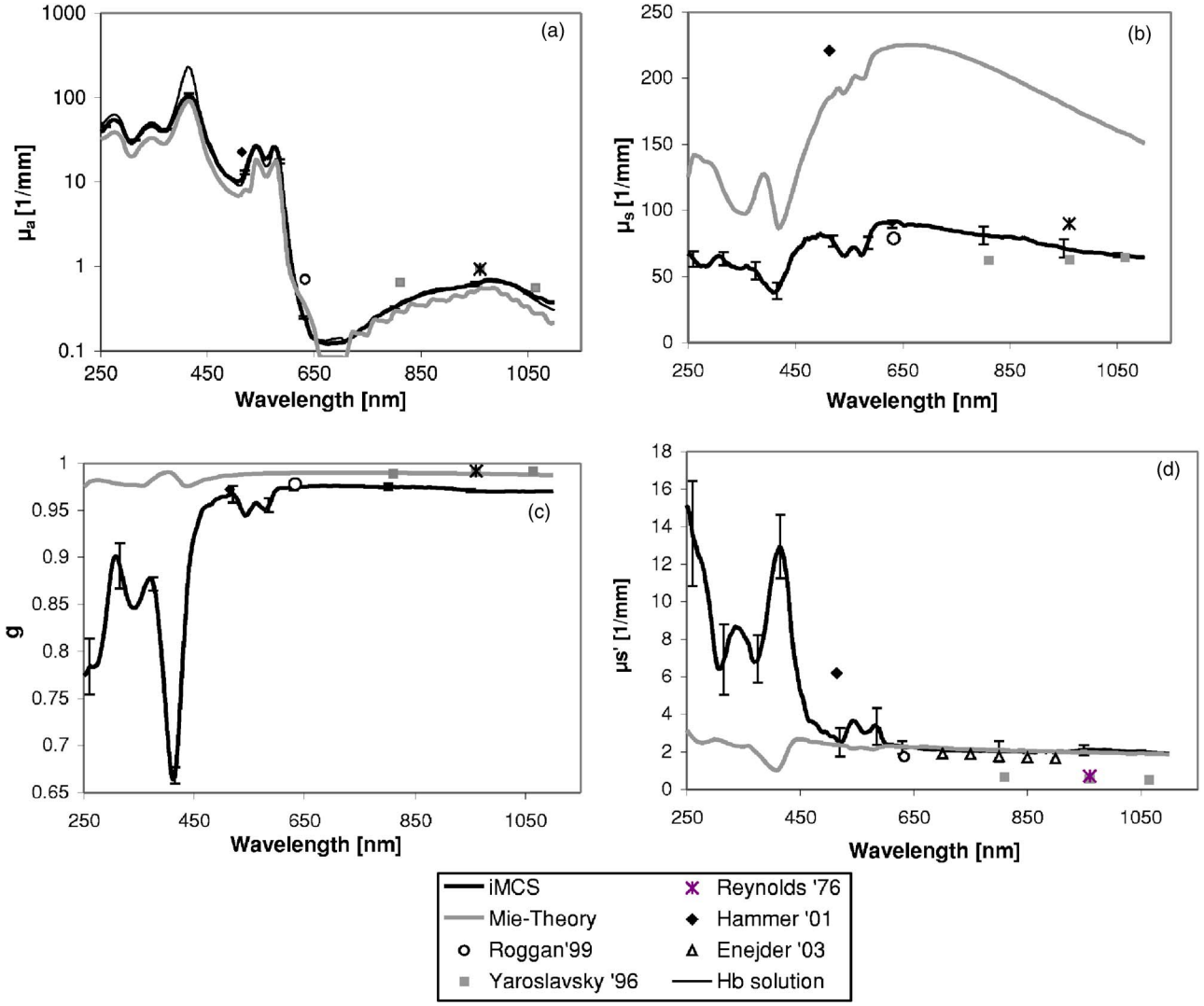

Fig. 6 (a) Absorption coefficient μ_a, (b) scattering coefficient μ_s, (c) anisotropy factor g, and (d) reduced scattering coefficient μ_s' of flowing red blood cells (wall shear rate 600 s^{-1}) with a hematocrit value of 42.1% in the wavelength range 250 to 1100 nm, compared to μ_a of a hemoglobin solution (12.9 g/dL), to values calculated by the Mie theory and to various data from the literature.[2,4,7,18,21]

means that the influence of wavelength, including changes in absorption over almost 4 orders of magnitude, can only be considered by adaptation of the anisotropy factor g. Changes in hematocrit leading to changes in occurrence of multiple scattering and interference phenomena needs the variation of both g and α. In principle, these results are in agreement with Hammer et al.,[9] who found the effective phase function $(\mathrm{RM}, \alpha = 1.5)$ for highly diluted blood wavelength independent in the spectral region 489 to 690 nm, including absorption changes by two orders of magnitude. The quite different phase function $(\mathrm{RM}, \alpha = 0.49)$ determined for nondiluted blood via angle-resolved IMCS at 514 nm also indicates concentration dependence.[21] In contrast to the results in this work, the variation factor α decreases with increasing blood concentration.

It should be mentioned that the MCS is based on the assumption of constant optical parameters in the considered area. Therefore, spatial variations in the Hct caused by flow dependent radial diffusion must be accounted for by the effective phase function. Consequently, the cuvette thickness combined with the Hct also has an influence on the evaluation of the effective phase function, because the radial diffusion, which leads to local inhomogenities in Hct, is dependent on the cuvette thickness.

3.5.2 *Comparison With Mie Theory*

For blood in physiological concentrations, the Mie theory offers a good description of the absorption coefficient in the range 600 to 1100 nm. In the spectral region of high absorption, the Mie theory underestimates μ_a, with maximal deviations of up to 35%. However, it fails to adequately describe the scattering parameters. There is only sufficient agreement for μ_s' in the wavelength range 600 to 1100 nm. This is not entirely unexpected with respect to the differences between flowing blood cells and single ideal spheres, and the conditions for applying the Mie theory. In addition to the nonspherical discoid shape of red blood cells, optically relevant

parameters such as hemoglobin content, mean cell volume, and hemoglobin concentration of an erythrocyte show a wide statistical range. For example, the volume of the cells ranges from 20 to 200 μm^3 and gives a mean cell volume of about 90 μm^3.

The mean distance between the cells even in diluted blood with a Hct of 0.84% is not large enough to ensure that the requirements of independent single scattering are fulfilled. Nilsson et al.[11] gave the boundary condition for independent scattering as a minimum of three times the radius of the scatterer. Under flow conditions, axial migration occurs where the cells tend to move into the center of a vessel or cuvette, inducing local inhomogenities in Hct. As a consequence, in undiluted blood, collective scattering becomes increasingly important.[20]

The Mie theory can only be used for calculating the anisotropy factor of flowing, highly diluted blood in spectral ranges where the hemoglobin absorption is low. With the cuvette thickness used for this hematocrit, axial migration is less pronounced than it is at the lower thickness used for the undiluted blood. The value for μ_s may be predicted at blood concentrations lower than Hct 0.84%, where the requirements for independent scattering are completely fulfilled. The most significant difference between the measured optical parameters and those predicted by the Mie theory, independent of Hct, is the fact that the anisotropy factor is found to be significantly influenced by the absorption of the scattering particle. As expected, the increase in the complex refractive index results therefore in an increase in the reflection and a decrease in transmittance, resulting in increased backscattering of the photons.

The Mie theory seems to exhibit this behavior, too, but at absorption values a hundred times higher, where the imaginary part of the refractive index predominates over the real part. This difference is due to the high anisotropic discoid shape of the red blood cells. This has been found in ongoing investigations. So far, it has been proven that when the erythrocytes were made to swell to more spheroid forms by reducing the osmolarity, they approximate the values given by the Mie theory. A reduction in the wall shear rate led to the same effect, because randomization of the cells increases, whereas alignment[5] and deformation of the cells decreases, leading to more spherical geometries. According to the investigation of Gandjbakhche et al.[15] and Bayer et al.,[6] the red blood cells should have a deformability index of approximately 0.2 and an elongation coefficient of 0.1 under the shear rate and viscosity conditions of the present experiments.

4 Conclusion

In this study, a high precision integrating sphere setup for measuring R_d, T_t, and T_d in combination with a high resolving IMCS is used to determine the intrinsic optical parameters of diluted and undiluted human blood under flow conditions in the wavelength range 250 to 1100 nm. Using a new algorithm, an appropriate effective phase function could be evaluated for both blood concentrations within the IMCS. Minimal errors in the simulation could be effected using the Reynolds-McCormick phase function with a variation factor $\alpha = 1.25$ for Hct 0.84% and $\alpha = 1.7$ for Hct 42.1%, respectively. Significant wavelength dependence of the variation factor is not observed. Using these evaluated effective phase functions, the intrinsic parameters μ_a, μ_s, and g of blood of physiological red blood cell concentration as well as for diluted blood are obtained separately in the whole of the spectral range, covering the high absorption bands of hemoglobin. A comparison with the Mie theory calculated for spheres of the same complex refractive index and mean volume showed that the Mie theory can generally be used for predicting the absorption coefficient in the wavelength range 600 to 1100 nm where μ_a is low. Using the frequently used approximation function $\mu_s = \mathrm{Hct}(1-\mathrm{Hct})(\sigma_s/V)$, the scattering coefficient may only be estimated by the Mie theory for highly diluted blood ($\ll$Hct 1%), and the anisotropy factor can only be predicted for diluted blood (Hct $\approx$ 1%) in the spectral range where the Hb absorption is low (600 to 1100 nm). For undiluted blood, only the effective scattering coefficient μ_s' can be estimated in the wavelength range 600 to 1100 nm. In the spectral range of high absorption, μ_s' is for both diluted and undiluted blood up to 12 times higher than values calculated by the Mie theory. The limitations of the Mie theory describing the optical properties of blood could be overcome by the use of the transport equation with an effective phase function. In contrast to the Mie theory, the use of the IMCS in combination with selected appropriate effective phase functions takes into consideration the nonspherical shape of the red blood cells, the phenomenon of coupled absorption and scattering, multiple scattering, and interference phenomena between close neighboring cells and inhomogeneous local distribution within the flow stream. Therefore, for the first time, reasonable results can be obtained for the optical behavior of human blood, even at high hematocrit and high hemoglobin absorption areas.

Acknowledgments

This work was supported by the Federal Ministry of Education and Research (grant number 13N7522). The authors wish to thank Stöckert Instrumente GmbH, Munich, for placing the equipment at our disposal. The blood bags were kindly provided by the research group of Kiesewetter, Institut für Transfusionsmedizin, Charité-Universitätsmedizin, Campus Mitte, Berlin, Germany.

References

1. M. Friebel and M. Meinke, "Determination of the complex refractive index of highly concentrated hemoglobin solutions using transmittance and reflectance measurements," *J. Biomed. Opt.* **10**, 064019 (2005).
2. A. Roggan, M. Friebel, K. Dörschel, A. Hahn, and G. Müller, "Optical properties of circulating human blood in the wavelength range 400–2500 nm," *J. Biomed. Opt.* **4**(1), 36–46 (1999).
3. L. G. Lindberg and P. A. Oberg, "Optical properties of blood in motion," *Opt. Eng.* **32**(2), 253–257 (1993).
4. A. M. K. Enejder, J. Swartling, P. Aruna, and S. Andersson-Engels, "Influence of cell shape and aggregate formation on the optical properties of flowing whole blood," *Appl. Opt.* **42**(7), 1384–1394 (2003).
5. V. S. Lee and L. Tarassenko, "Absorption and multiple scattering by suspensions of aligned red blood cells," *J. Opt. Soc. Am. A* **8**(7), 1135—1141 (1991).
6. R. Bayer, S. Çaglayan, and B. Günther, "Discrimination between orientation and elongation of RBC in laminar flow by means of laser diffraction," *Proc. SPIE* **2136**, 105–113 (1994).
7. A. N. Yaroslavsky, I. V. Yaroslavsky, T. Goldbach, and H. J. Schwarzmaier, "The optical properties of blood in the near infrared spectral range," *Proc. SPIE* **2678**, 314–324 (1996).

8. A. N. Yaroslavsky, I. V. Yaroslavsky, T. Goldbach, and H. J. Schwarzmaier, "Influence of the scattering phase function approximation on the optical properties of blood determined from the integrating sphere measurements," *J. Biomed. Opt.* **4**(1), 47–53 (1999).
9. M. Hammer, D. Schweitzer, B. Michel, E. Thamm, and A. Kolb, "Single scattering by red blood cells," *Appl. Opt.* **37**(31), 7410–7418 (1998).
10. A. N. Yaroslavsky, I. V. Yaroslavsky, T. Goldbach, and H. J. Schwarzmaier, "Different phase function approximations to determine optical properties of blood: A comparison," *Proc. SPIE* **2982**, 324–330 (1997).
11. A. Nilsson, P. Alsholm, A. Karlson, and S. Andersson-Engels, "T-matrix computation of light scattering by red blood cells," *Appl. Opt.* **37**(13), 2735–2748 (1998).
12. A. H. Gandjbakhche, P. Mills, and P. Snabre, "Light-scattering technique for the study of orientation and deformation of red blood cells in a concentrated suspension," *Appl. Opt.* **33**(6), 1070–1078 (1994).
13. A. Priezzhev, S. G. Khatsevich, and V. Lopatin, "Asymmetry of light backscattering from Couette flow of RBC suspensions: application for biomonitoring of blood samples," *Proc. SPIE* **3567**, 213–222 (1999).
14. V. Lopatin, A. Priezzhev, and V. Feodoseev, "Numerical simulation of light scattering in turbid biological media," *Crit. Rev. Biomed. Eng.* **29**(3), 400–419 (2001).
15. A. H. Gandjbakhche, A. Othmane, P. Mills, P. Snabre, and J. Dufaux, "Aggregation and deformation of red blood cells as probed by a laser light scattering technique in a concentrated suspension: Comparison between normal and pathological blood cells," *Proc. SPIE* **2136**, 97–104 (1994).
16. A. Priezzhev, O. M. Ryaboshapka, N. N. Firsov, and I. V. Sirko, "Aggregation and disaggregation of erythrocytes in whole blood: study by backscattering technique," *J. Biomed. Opt.* **4**(1), 76–84 (1999).
17. J. Lademann, H. Richter, W. Sterry, and A. V. Priezzhev, "Diagnostic potential of erythrocytes aggregation and sedimentation measurements in whole blood," *Proc. SPIE* **4263**, 106–111 (2003).
18. L. Reynolds, "Diffuse reflectance from a finite blood medium: application to the modelling of fiber optic catheter," *Appl. Opt.* **5**, 2059–2067 (1976).
19. J. M. Steinke and A. P. Sheperd, "Comparision of Mie theory and light scattering of red blood cells," *Appl. Opt.* **27**(19), 4027—4033 (1988).
20. D. J. Faber, F. J. van der Meer, M. C. G. Aalders, D. M. de Bruin, and T. G. van Leeuwen, "Hematocrit-dependence of the scattering coefficient of blood determined by optical coherence tomography," *Proc. SPIE* **5861**, 58610W (2005).
21. M. Hammer, A. N. Yaroslavsky, and D. Schweitzer, "A scattering phase function for blood with physiological haematocrit," *Phys. Med. Biol.* **46**, N65–N69 (2001).
22. M. Meinke, I. Gersonde, M. Friebel, J. Helfmann, and G. Müller, "Chemometric determination of blood parameters using visible-near-infrared spectra," *Appl. Spectrosc.* **59**(6), 826–835 (2005).
23. A. Roggan, O. Minet, C. Schröder, and G. Müller, "Measurements of optical tissue properties using integrating sphere technique," *Medical Optical Tomography: Functional Imaging and Monitoring*, Vol. **IS11**, pp. 149–165, SPIE Press, Bellingham, WA (1993).
24. W. H. Press, B. P. Flannery, S. A. Teukolskyc, and W. T. Vetterling, *Numerical Recipes in Pascal*, Cambridge University Press, Cambridge, MA (1989).
25. G. Mie, "Pioneering mathematical description of scattering by spheres," *Ann. Phys.* **25**, 337 (1908).
26. L. G. Henyey and J. L. Greenstein, "Diffuse radiation in the galaxy," *Astrophys. J.* **93**, 70–83 (1941).
27. R. N. Pittman, "In vivo photometric analysis of hemoglobin," *Ann. Biomed. Eng.* **14**, 119–137 (1986).
28. M. Friebel and M. Meinke, "Model function to calculate the refractive index of native hemoglobin in the range of 250–1100 nm dependent on concentration," *Appl. Opt.* **45**(12), 2838–2842 (2006).
29. V. Twersky, "Absorption and multiple scattering by biological suspensions," *J. Opt. Soc. Am.* **60**, 1084–1093 (1970).